

1 **Antimicrobial resistance gene shuffling and a three-element mobilisation system in the**
2 **monophasic *Salmonella* Typhimurium strain ST1030**

3
4 Oliva M.¹, Calia C.¹, Ferrara M.², D'Addabbo P.¹, Scrascia M.¹, Mulè G.², Monno R.³, Pazzani C.^{1*}

5
6 ¹ Department of Biology, University of Bari, via Orabona, 4, 70125 Bari, Italy

7 ² Institute of Sciences of Food Production, National Research Council of Italy (ISPA-CNR), Via G.
8 Amendola 122/O, 70126 Bari, Italy

9 ³ Department of Basic Medical Sciences Neurosciences and Sense Organs Medical Faculty,
10 University of Bari Piazza G. Cesare Policlinico, 70124 Bari, Italy

11
12 * Author to whom correspondence should be addressed

13 Carlo Pazzani

14 carlo.pazzani@uniba.it

15 Tel.: +39 080 5443379

16 **Keywords**

17 monophasic variant 1,4,[5],12:i:-; IS26; Tn21-derived; I1 conjugative; ColE1-like; orphan mob-
18 associated *oriT*.

Abstract

19

20 In this study we describe the genetic elements and the antimicrobial resistance units (RUs)
21 harboured by the *Salmonella* Typhimurium monophasic variant 1,4,[5],12:i:- strain ST1030. Of the
22 three identified RUs two were chromosomal, RU1 (IS26-*bla*_{TEM-1}-IS26-*strAB-sul2*- IS26) and RU2
23 (IS26-*tetR*(B)-*tetA*(B)- Δ IS26), and one, RU3 (a *sul3*-associated class 1 integron with cassette array
24 *dfrA12-orfF-aadA2-cmlA1-aadA1*), that was embedded in a Tn21-derived element harboured by the
25 conjugative II plasmid pST1030-1A. IS26 elements mediated the antimicrobial resistance gene
26 (ARG) shuffling and this gave rise to pST1030-1A derivatives with different sets of ARGs. ST1030
27 also harboured two ColE1-like plasmids of which one, pST1030-2A, was mobilisable and the target
28 of an intracellular translocation of the Tn21-derived element; the second (pST1030-3) was an
29 orphan *mob*-associated *oriT* plasmid co-transferred with pST1030-1A and pST1030-2A. pST1030-
30 2A and pST1030-3 also carried a *parA* gene and a type III restriction modification system,
31 respectively. Overall analysis of our data reinforces the role played by IS26, Tn21-derived elements
32 and non-conjugative plasmids in the spread of ARGs and supplies the first evidence, at least in
33 *Salmonella*, for the identification of a natural isolate harbouring a three-element mobilisation
34 system in the same cell.

35 ***1. Introduction***

36 Genetic elements such as insertion sequences (IS), transposons (Tn) and plasmids play a key
37 role in the spread of antimicrobial resistance genes (ARGs) (Partridge et al., 2018). Among the IS,
38 IS26 plays a leading role in the mobilisation and spread of ARGs. In Gram-negative bacteria, IS26
39 has been detected in chromosomes, Tn, and plasmids and associated with different ARGs (Harmer
40 and Hall, 2015; He et al., 2015; Mollet et al., 1985; Moran and Hall, 2017; Oliva et al., 2018). IS26
41 can move by a replicative mechanism which, when causing deletions of adjacent sequences,
42 generates the so-called translocatable unit (TU) (Harmer et al., 2014). Integration of TU can occur
43 through either an untargeted replicative (random insertion) or a conservative (targeting other IS26
44 elements) mechanism (Harmer and Hall, 2016). The latter is responsible for the formation of
45 multimeric arrays of IS26 flanking DNA sequences (Harmer and Hall, 2017). In addition, the gene
46 shuffling mediated by IS26 within and between genetic elements triggers the arrangement of
47 different sets of ARGs that might be horizontally transferable.

48 Among the Tn, Tn21 and its derivatives have an important role in HGT in that they are
49 widespread and harbour a large range of ARGs (Liebert et al., 1999). In Tn21 and its derivatives
50 ARGs are generally embedded in class 1 integrons (the class more broadly distributed in
51 Proteobacteria), which are genetic elements able to integrate and express gene cassettes (Cambray
52 et al., 2010; Domingues et al., 2015; Hall and Collis, 1995; Stokes and Gillings, 2011). In Tn21
53 derivatives an IS26 is often found within class 1 integrons at the end of the 3'-conserved segment
54 (3'-CS) (*sull*, *qacEΔ1* and *orf5*) interrupting the *tniA* gene (Moran and Hall, 2018). The junction
55 between IS26 and the remainder of *tniA* is conserved in both class 1 integrons containing *sull* and
56 the 3'-CS, and in the rarer *sul3*-associated class 1 integrons where the 3'-CS was replaced by the
57 *sul3*-segment (*tnp440-sul3-orf1-IS26*) (Antunes et al., 2007; Curiao et al., 2011; Moran et al.,
58 2016). The linkage among Tn21-derivative elements, class 1 integrons and conjugative plasmids
59 and its relevance in HGT of ARGs has been widely documented (Partridge et al., 2009; Stokes and
60 Gillings, 2011; Zheng et al., 2020). In *Salmonella*, an important foodborne pathogen, these elements

61 have frequently been detected in FI, FII, HI1 and I1 plasmids (Cain and Hall, 2012; Miriagou et al.,
62 2006; Oliva et al., 2018).

63 Conjugative plasmids that possess both relaxase and type IV secretion systems (T4SS)
64 represent only 28% of the plasmids identified in Proteobacteria (Smillie et al., 2010). In addition to
65 these plasmids, those classified as mobilisable can also contribute to the HGT of ARGs or, not least,
66 as a reservoir of ARGs. Subclassification of non-conjugative plasmids has recently been revised and
67 the identification of specific genetic features that allow their mobilisation has contributed to further
68 extending the potential role played by these genetic elements in the HGT (Ramsay and Firth, 2017).
69 In this study we describe: i) the plasmid content (I1 and ColE1-like) harboured by the multidrug-
70 resistant *S. Typhimurium* monophasic variant (STMV) 1,4,[5],12:i:- strain ST1030; ii) the ARG
71 shuffling and their HGT; iii) the mobilisation of the detected two detected pST1030-2A and
72 pST1030-3 ColE1-like plasmids (of which pST1030-3 was an orphan *mob*-associated *oriT*)
73 (Ramsay and Firth, 2017), mediated by the conjugative pST1030-1A I1 plasmid.

74

75 **2. Materials and methods**

76 *2.1 Bacterial isolates and antimicrobial susceptibility testing*

77 The STMV ST1030 is a clinical strain isolated in Southern Italy in 2008 (De Vito et al.,
78 2015). ST1030 was assigned to the monophasic variant 1,4,[5],12:i:- on the basis of the absence of
79 the *fljB* gene tested by PCR (Echeita et al., 2001). Antimicrobial susceptibility tests were performed
80 as reported previously (Oliva et al., 2017). The antimicrobials were: ampicillin (Ap),
81 chloramphenicol (Cm), streptomycin (Sm), sulphamethoxazole (Su), tetracycline (Tc) and
82 trimethoprim (Tp).

83

84 *2.2 Bacterial conjugation, gene detection, plasmid typing and kinetic growth*

85 Conjugation experiments were performed at 37 °C as described previously (Oliva et al.,
86 2018). Antimicrobial concentrations used were: Ap 100 µg/mL, Cm 25 µg/mL, nalidixic acid (Nx)

87 50 µg/mL, rifampicin (Rf) 100 µg/mL, Sm 100 µg/mL, Su 600 µg/mL, Tc 20 µg/mL, Tp 30 µg/mL.
88 Nalidixic acid-resistant CSH26 Nal or rifampicin-resistant DH5α Rf *Escherichia coli* strains were
89 used as recipients. The frequency of transfer, mean number of transconjugants per donor, was
90 determined in three or more independent experiments and the standard deviation (SD) calculated
91 (Table 1). Plasmids were typed by the PCR Based Replicon Typing protocol (PBRT) using positive
92 controls kindly supplied by A. Carattoli (Carattoli et al., 2005). Detection of ARGs, genetic
93 elements and gene organization were performed by PCRs on ST1030, transconjugants and
94 transformants. Primers used in this study were as reported previously (Camarda et al., 2013; Oliva
95 et al., 2018) or newly designed (Table S1).

96

97 *2.3 DNA sequencing, assembly and annotation*

98 Total genomic and plasmid DNA were extracted was extracted by the cetyl
99 trimethylammonium bromide method (Murray and Thompson, 1980). About 1 µg of DNA was
100 sheared with a Covaris M220 Focused-ultrasonicator (Covaris, Inc., MA, USA) with a target size of
101 400 bp and used for library preparation with the Ion Xpress Plus gDNA Fragment Library kit (Life
102 Technologies, USA), following the manufacturer's instructions. Size selection of libraries (~400 bp)
103 were performed by agarose gel electrophoresis using 2% E-Gel SizeSelect Agarose Gels (Life
104 Technologies, USA). After purification, library concentrations were quantified using the Qubit
105 dsDNA HS Assay Kit (Life Technologies, USA). Template-positive Ion Sphere Particles were
106 prepared for 400-base-read using the Ion OneTouch 2 System (Thermo Fisher Scientific, Carlsbad,
107 CA, USA) with an Ion 520 & 530 Kit-OT2 (ThermoFisher Scientific, USA) and then sequenced on
108 an Ion 530 Chip using an Ion S5 System (ThermoFisher Scientific, USA). Raw data were quality
109 filtered and assembled by using SPAdes assembler version 3.10.1 (Bankevich et al., 2012).

110 Contigs were assembled by specific PCRs and analysis of restriction profiles generated by
111 specific enzymes (Fig. 4, Fig. S1 and Table S2). The genetic organization of pST1030-1B and
112 pST1030-1C was deduced by comparing their *ClaI*, *HindIII* and *XhoI* profiles with those of

113 pST1030-1A, and by specific PCRs. DNA sequences of pST1030-1A, pST1030-1B, pST1030-1C,
114 pST1030-2A, pST1030-2B, pST1030-3 and the chromosomal region spanning from STM2746 to
115 *iroC* (where the RU1 and RU2 were located) were deposited in GenBank under accession numbers
116 MT507877, MT507880, MT507879, MT507878, MT507883, MT507881 and MT507882,
117 respectively. STM refers to chromosomal genes as reported in *S. Typhimurium* referring strain LT2.
118 DNA sequences of pST1030-1A derivatives can be obtained by IS26-mediated ARG shuffling (for
119 details see section 3.3.1). DNA sequence of pST1030-2B was obtained by insertion of the Tn21-
120 derived element (harboured by pST1030-1A) into pST1030-2A (for details see section 3.4).

121 Annotation was automatically performed using PROKKA (Seemann, 2014) and edited on
122 the basis of its comparison with the well-characterised plasmids R64 (AP005147), ColIb-P9
123 (AB021078), pST1007-1A (MH257753), ColE1 (NC_001371) and NTP16 (L05392) and the
124 chromosomal region of ST1007 (MH257754). Gene nomenclature for pST1030-1A was as that
125 reported for R64 (Sampei et al., 2010).

126 Kinetics of bacterial growth were performed as follows: o/n cultures of strains grown in
127 Luria Bertani broth (LB) were diluted (1:10⁴) in 100ml (T₀) of LB in shake flasks and incubated at
128 37°C. Samples were collected every hour (T₁ to T₈) and serial dilutions were plated on LB agar
129 plates to assess the number of viable cells. The generation time (T_{gen}, time required to achieve a
130 doubling of the population size) was estimated by determining the cell number (N) during the
131 exponential phase (t) of active cell division and mathematically expressed using the following
132 equation:

$$133 T_{\text{gen}} = t \log 2 / (\log N_t - \log N_0).$$

134

135 2.4 Bioinformatic analysis

136 Similarity searches were performed using the BLASTN algorithm of the NCBI Web BLAST
137 (<https://blast.ncbi.nlm.nih.gov/Blast.cgi>) using the pST1030-1A, pST1030-2A and pST1030-3
138 sequences as query. Results were graphically depicted by SnapGene (<http://www.snapgene.com/>)

139 and Adobe Illustrator (<https://www.adobe.com/it/>). Putative promoter sequences were predicted
140 using the tool for promoter search in prokaryotic genomes (<http://www.phisitr.org/>) (Klucar et al.,
141 2010). Secondary structures of single stranded RNA or DNA sequences were predicted through the
142 ViennaRNA Web Services (<http://tbi.univie.ac.at/RNA/>) (Gruber et al., 2008; Lorenz et al., 2011).
143 Multiple sequence alignments were performed through the tool “MUSCLE”
144 (<https://www.ebi.ac.uk/Tools/msa/muscle/>) (Madeira et al., 2019).

145

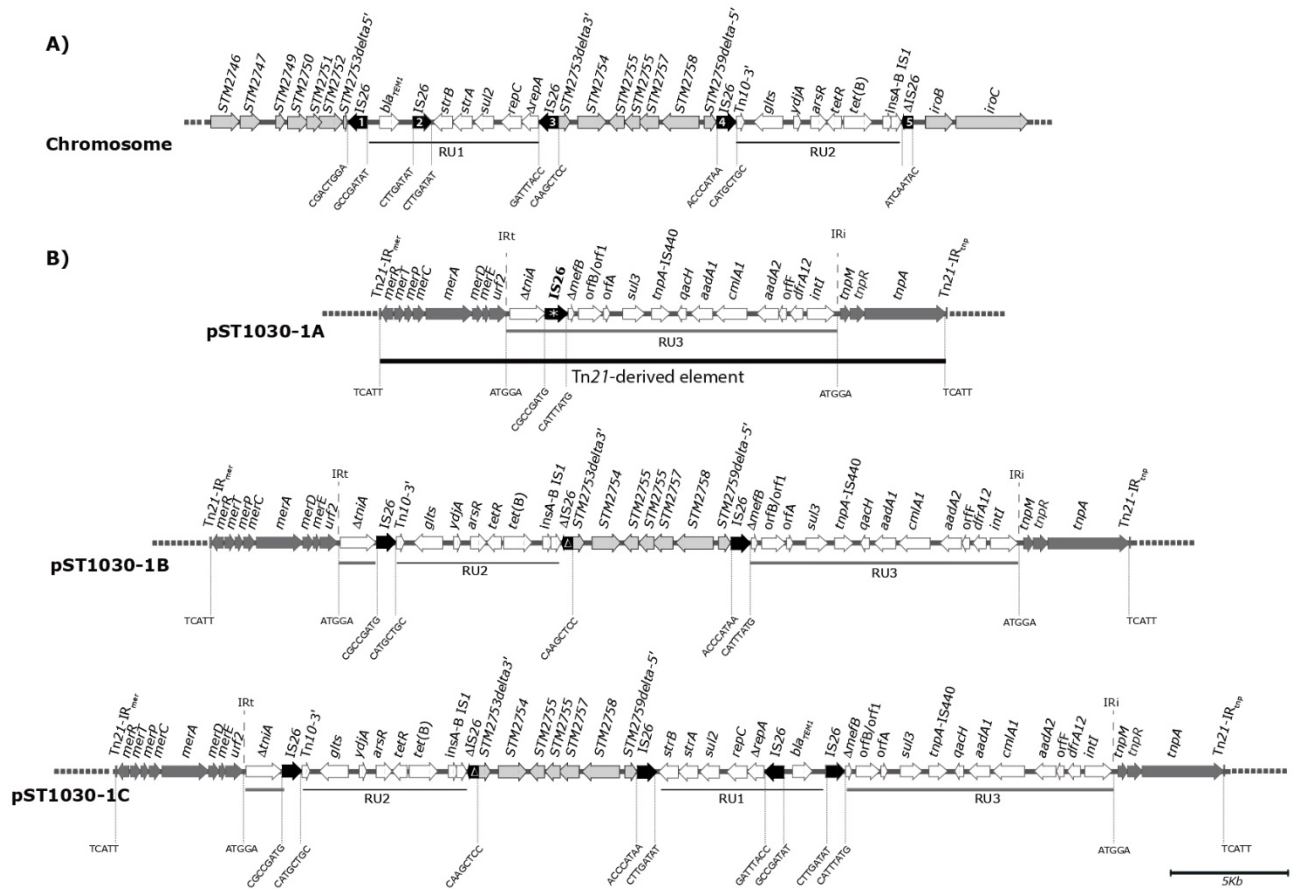
146 **3. Results**

147 *3.1 Genome sequence of ST1030 and context of resistance genes*

148 ST1030 is an STMV isolate which is part of a collection of 113 clinical MDR *S.*
149 Typhimurium strains isolated in Italy between 2006 and 2012 (De Vito et al., 2015). Analysis of the
150 ST1030 genome sequence revealed that in addition to the chromosome, three extrachromosomal
151 replicons were detected: a conjugative II (pST1030-1A) and two mobilisable ColE1-like (pST1030-
152 2A and pST1030-3) plasmids.

153 The ApCmSmSuTcTp resistance pattern, exhibited by ST1030, was encoded respectively by
154 *bla*_{TEM-1}, *cmlA1*, (*aadA1*, *aadA2*, *strAB*), (*sul2*, *sul3*), *tetR(B)-tetA(B)* and *dfrA12* genes organised
155 into three resistance units (RUs) (Fig. 1).

156



157

158

159

160

161

162

163

164

165

166

167

168

169

170

171

Fig. 1. Genomic localisation of resistance units (RUs) in ST1030

Genes and open reading frames are shown as arrows pointing in the direction of transcription. RUs and chromosomal genes are indicated with white and light grey arrows, respectively. Dark grey arrows delimit the extent of the Tn21-derived elements flanking the RUs. Strait thin black lines indicate RU1 and RU2. The thick grey and black lines indicate the *sul3*-associated class 1 integron (RU3) and the extent of the Tn21-derived element, respectively. The sequence and position of both the 8-bp flanking the IS26 and the target site duplications are indicated in capital letters. **A)** Chromosomal region harbouring RU1 and RU2 (GeneBank accession number MT507882). IS26 are numbered and indicated with black arrows. The IS26 number 5 is a Δ IS26, it lacks 129 bp that include both 77 bp 3'-*tnp26* and IRR. **B)** Linear representation of the distinguishing features between pST1030-1A and its derivatives. The IS26 present in pST1030-1A is marked with an asterisk (*). The Δ IS26, is shown with the symbol delta (Δ).

172

RU1 and RU2 were localised in the chromosome and flanked by IS26 (Fig. 1A). RU1

173

(IS26₁-*bla*_{TEM-1}-IS26₂-*strAB-sul2*- IS26₃), a Tn6029E (a variant of Tn6029) (Reid et al., 2015), was

174

inserted into STM2753; RU2 (IS26₄-*tetR(B)-tetA(B)*-IS1- Δ IS26₅), which contains regions derived

175

from Tn10 (Foster et al., 1981), was inserted into STM2759. The two IS26 flanking RU1 were

176

directly oriented; while those flanking RU2 were inversely oriented. The chromosomal region

177 between IS26₃ and IS26₄ could be found in both possible orientations: 3' STM2753-5' STM2759 or
178 5' STM2759-3' STM2753 (this was demonstrated by PCR and enzyme restrictions of amplicons,
179 Table S2). Similarly to what has been reported for the *S. Typhimurium* strain ST1007 (Oliva et al.,
180 2018), RU1 and RU2 of ST1030 were found integrated in the same position in STM2753 (with the
181 same 322 bp deletion of this gene) and ST2759, respectively. The Δ IS26₅ lacked 129 bp that
182 included the 77 bp 3'-*tnp26* and the IRR; this was demonstrated by PCR and sequencing of the
183 DNA amplicon (Fig. S1 and Table S2). The *iroB* gene was found next to Δ IS26₅. The chromosomal
184 region from 3' STM2759 to *fljA-fljB-hin* was missing and this accounted for the monophasic variant
185 of ST1030.

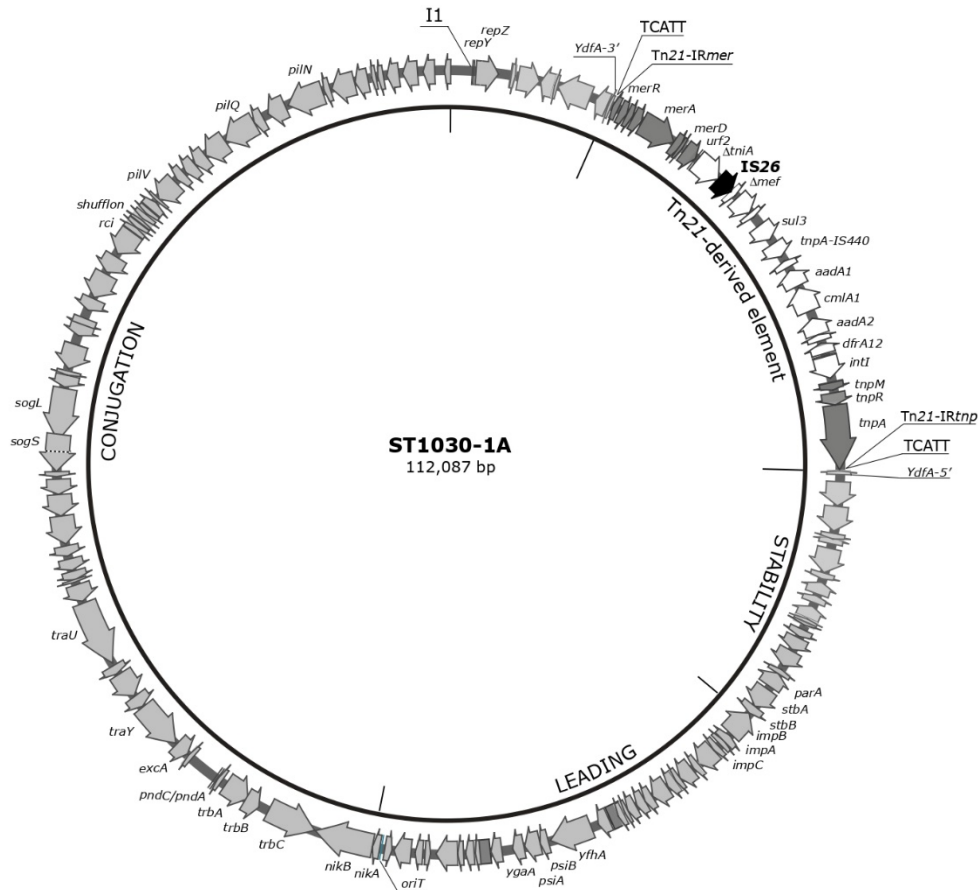
186 RU3 included a *sul3*-associated class 1 integron with the cassette array *dfrA12-orfF-aadA2-*
187 *cmlA1-aadA1*, that was embedded in a Tn21-derived element harboured by pST1030-1A (Fig. 1B).
188 The *sul3*-associated class 1 integron was flanked by imperfect inverted repeats of 25-bp (IRi and
189 IRt), bounded by a 5-bp direct duplication of the target site and inserted in the same position as In2
190 in Tn21 (Liebert et al., 1999). RU3 also contains an IS26 element inserted between the truncated
191 *mefB* and *tniA* genes.

192

193 3.2 ST1030's II plasmids

194 pST1030-1A consisted of 112,087 bp and comprised of a 91,242 bp backbone (50% GC),
195 the 20,840 bp Tn21-derived element and a 5 bp target site duplication (TSD) generated by insertion
196 of a Tn21-derived element into the backbone (Fig. 2). The pST1030-1A assembly was confirmed by
197 comparing its restriction profiles obtained with *ClaI*, with the patterns generated by *in silico*
198 restriction of its DNA sequence (Table S3). The pST1030-1A genome is organised into five major
199 functional regions: replication, drug resistance, stability, leading and transfer. The complete genome
200 sequences of R64 (AP005147) (Sampei et al., 2010) and ColIb-P9 (AB021078), the prototypes of
201 the IncII group plasmids, were used for comparison.

202



203

204

205 **Fig. 2.** Circular map of pST1030-1A

206 pST1030-1A is drawn to scale (GeneBank accession number MT507877). Genes and open reading
 207 frames are shown as arrows pointing in the direction of transcription. Only some genes or operons
 208 are labelled. Genes associated with replicative, stability, leading and conjugative regions are in light
 209 grey. Dark grey arrows flank the *sul3*-associated class1 integron (white arrows) and delimit the
 210 extend of the Tn21-derived element. The back arrow highlights the IS26. The target site duplication
 211 sequence is shown in capital letters

212

213

The replication region was very similar to R64 and ColIb-P9 with nucleotide identities of

214

100% for *inc* and *repY*; and 94% for *repZ*. The drug resistance region included the *sul3*-associated

215

class 1 integron embedded in the Tn21-derived element. The *sul3*-associated class 1 integron was

216

similar to that identified in pCERC3 (a ColV virulence-multidrug resistance plasmid isolated from a

217

commensal *E. coli* strain) (Moran et al., 2016) and identical to that detected in pST1007-1A (a

218

mosaic conjugative FII plasmid isolated from the clinical MDR *S. Typhimurium* strain ST1007)

219

(Oliva et al., 2018). As in the case of pST1007-1A, the Tn21-derived element of pST1030-1A was

220

inserted into *ydfA* (generating a 5-bp direct duplication) and contained a single copy of IS26 while

221 the Tn21-derived element harboured by pST1007-1A contained a second IS26 element inserted into
222 the *tnpR* of the Tn21-module. The stability region contained few homologies with the stability
223 regions of R64 or pColIb-P9. These homologies were mainly restricted to *orfs* next to pST1030-1A
224 *oriV*. However, when the stability region of pST1030-1A was searched as a query in GenBank
225 sequences, it proved to be nearly identical ($\geq 90\%$, with query cover of 100%) to other IncI1
226 plasmids detected in *S. Typhimurium*, STMV and *E. coli* strains (accession numbers JF274993,
227 JQ901381, CP030921, CP039604, LT95504). The stability region of pST1030-1A ended with the
228 partitioning system *stbA-stbB*. The leading region was similar (nucleotide identity ranging from 95
229 to 99%) to those of R64 and ColIb-P9. A notable difference was that shared for *ygaA*: homologous
230 only with R64; ColIb-P9 contained *ydcA* rather than *ygaA*.

231 pST1030-1A *oriT* was nearly identical (81/83 nt) to the minimal sequence of R64 *oriT*
232 (Furuya and Komano, 1997). The two mismatches detected in pST1030 *oriT* were complementary
233 to each other in the formation of the stem-loop of the 17 bp inverted repeat involved in the
234 termination of DNA transfer (Fig. S2). The gene organization of the transfer region was similar to
235 R64 and ColIb-P9 with a nucleotide identity ranging from 97 to 99%. Lower identities were
236 detected for *excA* (75% restricted to the 501nt 3' end) and *traY* (86% over the entire gene with 72%
237 identity restricted to the 1066 nt 3' end). The *traD* of R64 was not detectable and, in its place, an *orf*
238 identical to *trcD* of ColIb-P9 was found. The shufflon region of pST1030-1A contained the four
239 segments A, B, C and D found in R64 (Brouwer et al., 2015).

240 Results by searching and aligning GenBank sequences, using the pST1030-1A sequence as
241 query detected no identical plasmids. The most similar plasmids (coverage $>95\%$ and identity
242 $>98\%$) were: pSal8934a (JF274993), p12-6919.1 (CP039604), II (LT795504), Plm (JQ901381),
243 pS68 (KU130396), A (CP010130), pUY_STM96 (MN241905), pUR-EC07 (MH674341). Plasmids
244 were isolated from *E. coli*, *S. Typhimurium* or STMV. Interestingly, these plasmids harboured a
245 nearly identical fragment previously described in pST1007-1A and name fragment C. However,
246 none of the detected II plasmids (apart from the plasmid II), contained a Tn21-derived element

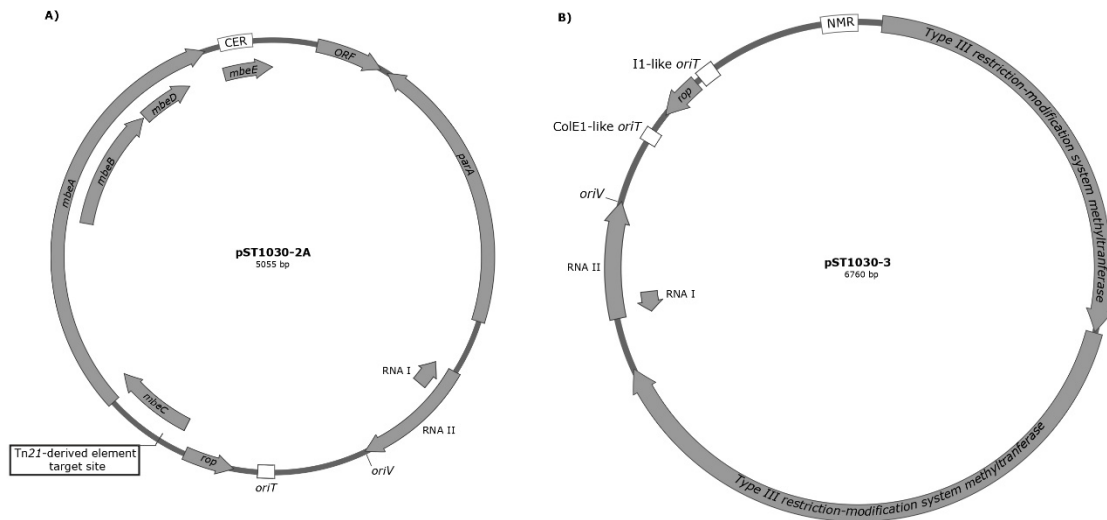
247 inserted within the fragment C. In plasmid II the Tn21-derived element was not inserted into *ydfA*
248 but into *ydfB*. The Tn21-derived element of plasmid II was nearly identical to the Tn21-derived
249 element harboured by pST1030-1A. It differed only in 3 nucleotide mismatches of which one was
250 localised in the *tnp26* (replacement of the leucine in position 110 of Tnp26 by an isoleucine), the
251 other two were found in the genes *aadA1* and *tnpA* of the Tn21, respectively. These last mismatches
252 were in the third base and did not affect the amino-acid sequences.

253 pST1030-1B and pST1030-1C were from insertion of IS26-mediated TUs originated from
254 the chromosomal RUs (Fig. 1B): TU1 derived through recombination of the two directly orientated
255 IS26 (IS26₁ and IS26₃) that flanked RU1; TU2 through recombination of the two directly orientated
256 IS26 (IS26₃ and ΔIS26₅) that encompassed RU2 and the chromosomal gene cluster 3'STM2753 -
257 5'STM2759 (Fig. 1A). Insertion of TU2 into the IS26 present in the Tn21-derived element of
258 pST1030-1A accounted for the formation of pST1030-1B. For pST1030-1C two possible molecular
259 processes have been hypothesised: i) insertion of TU1 into pST1030-1B; ii) insertion of the
260 cointegrated TU1-2 (generated by recombination between TU1 and TU2) into pST1030-1A. It is
261 noteworthy that detection of transconjugants harbouring either pST1030-1B or pST1030-1C was
262 rare (mean frequency of 4.4 x 10⁻⁸ and 6.6 x 10⁻⁹ TC/D, respectively) (see paragraph 3.4). Tnp26-
263 catalysed exchange between IS26 elements occurs via crossover between either the two left or the
264 two right ends of the IS elements (Harmer and Hall, 2017). In the case of TU2 recombination
265 between ΔIS26₅ and IS26₃ could only happen between the two left ends, leaving an integral IS26 on
266 the chromosome and the ΔIS26₅ in the TUs (this was demonstrated by PCR and enzyme restrictions
267 of amplicons, Fig. S1 and Table S2).

268

269 3.3 ST1030's *ColE1*-like plasmids

270 The pST1030.2A and pST1030-3 *ColE1*-like plasmids consisted of 5,055 and 6,760 bp,
271 respectively (Fig. 3). The complete sequences of the widely studied *ColE1* (Chan et al., 1985) and
272 NTP16 (Cannon and Strike, 1992) plasmids were used for comparison.



274

275

276 **Fig. 3.** Circular map of pST1030-2A and pST1030-3

277 Genes and open reading frames are shown as arrows pointing in the direction of transcription and,
 278 for each plasmid, genes are to scale. **A)** pST1030-2A (GeneBank accession number MT507878).
 279 The multimeric resolution (*cer*) and *oriT* sites are in white boxes. Vertical bars indicate the origin of
 280 replication (*oriV*) and the site of insertion of the Tn21-derived element that originated pST1030-2B.
 281 **B)** pST1030-3 (GeneBank accession number MT507881). The multimeric resolution (*nmr*), and
 282 ColeE1-like and I1-like *oriT* sites are in white boxes. The vertical bar indicates the origin of
 283 replication (*oriV*).
 284

285 pST1030-2A comprises a backbone of ~3,3 kb and a variable region of ~1,7 kb. The
 286 backbone was composed of the regions: mobilisation (*mbeA*, *mbeB*, *mbeC*, *mbeD*, *mbeE* and *oriT*),
 287 replication (*oriV* and *rop*) and recombination. *rop* of pST1030-2A was 98% identical to *rop* of
 288 ColeE1. ST1030-2A *oriT* was 98.7% identical in 79 bp overlap with the 83bp minimal length of
 289 ColeE1 *oriT* (Varsaki et al., 2009). The recombination region was comparable to the *cer* site of
 290 ColeE1, sharing an identical *Arg-box* sequence and similar XerC (3 nucleotide mismatches) and
 291 XerD (3 nucleotide mismatches) binding sites (Fig. S3). The variable region contains the gene
 292 *parA*. The predicted ParA protein is a member of the P loop GTPase superfamily, SIMIBI class
 293 (Leipe et al., 2002). In particular, ParA of pST1030-2A is ascribable to the distinct subgroup called
 294 “orphan ParAs” (Lutkenhaus, 2012). Orphan ParAs are not associated with the usual partner ParB
 295 and are characterised by the “deviant Walker A motif – XKGGXXK[T/S]” that contains two

296 conserved lysines of which the second is common to all walker motifs and required for binding and
297 hydrolysis of ATP; the amino terminal lysine, called “lysine signature”, is unique to this subgroup
298 (Lutkenhaus and Sundaramoorthy, 2003).

299 pST1030-2B, as deduced by analysis of both its DNA sequence and restriction profiles,
300 derived from insertion of the Tn21-derived element into *mbeC* of pST1030-2A (Fig. 3). The
301 insertion resulted in a 5-nt (5'-TACTT-3') duplication of the target site and *mbeC* was split into a
302 5'-segment of 69-bp and a 3'-segment of 284-bp (referred to as $\Delta mbeC$). Insertion of the Tn21-
303 derived element also generated the sequence 5'-CCTACT-3' (overlapping the IR-Tn21 and the 5 bp
304 target site) that is consistent with a putative -10 sequence promoter. The 5'-TTTCCG-3' sequence
305 (putative -35 sequence promoter) found 15 bp upstream of the -10 sequence, generated a potential
306 new promoter (Shimada et al., 2014). Putative transcription and translation of $\Delta mbeC$ would have
307 produced a $\Delta MbeC$ of 81aa that retained the conserved amino acid domain (aa 26 to 68) of the
308 superfamily bacterial mobilisation protein MobC and the NLN motif possibly involved in the
309 interaction with any of the proteins implicated in conjugal mobilisation (Marchler-Bauer et al.,
310 2017; Varsaki et al., 2009). MbeC has been hypothesised to interact through its C-terminal region
311 with the N-terminal region of the MbeA relaxase, guiding MbeA to the *nic* site of *oriT*. MbeC also
312 retains an additional functional motif (ribbon-helix-helix) localised in its N-terminal region that
313 would recognise a DNA sequence of *oriT* next to the *nic* site (Varsaki et al., 2012). Therefore, it has
314 been suggested MbeC plays a role in the efficient mobilisation of ColE1.

315 pST1030-3 comprises a backbone of ~1,9 kb and a variable region of ~4,8 kb (Fig. 3). The
316 backbone was composed of the regions: replication (*oriV* and *rop*), transfer (*oriT*) and
317 recombination. There was 67.4% identity (in 184 bp) between *rop(s)* of pST1030-3 and pST1030-
318 2A with an amino acid sequence homology of 78% over the entire proteins. ST1030-3 *oriT* was
319 93.1% identical in 72 bp overlap with the 83bp minimal length of ColE1 *oriT* (Varsaki et al., 2009).
320 Next to *rop*, pST1030-3 contains a region of 82 bp similar (85.4% identity) to the *oriT* sequences of
321 both R64 and pST1030-1A. This region included the sequences recognised by R64 NikA. The

322 recombination region was comparable to the *nmr* site of NTP16, sharing an identical *Arg-box*
323 sequence and a very similar XerC (1 nucleotide mismatch) and XerD (1 nucleotide mismatch)
324 binding sites (Fig. S3). The variable region contains two ORFs of 1866 and 2637 bp encoding for
325 putative type III N6-adenine DNA methyltransferase (M) and Type III restriction (R), respectively
326 (Roberts et al., 2015).

327 Replication of ColE1 plasmids is mediated by an RNA pre-primer (RNA II) that forms a
328 stable hybrid with the DNA in the origin region. Replication control is modulated by the antisense-
329 RNA (RNA I) which is transcribed from the complementary strand in the 5' pre-primer region
330 (Brantl, 2014; Camps, 2010). The RNAII of pST1030-2A and pST1030-3 share identity with the
331 RNAII of ColE1 and NTP16 only in the 3' terminal 360 bp. The respective RNAI sequences of
332 these plasmids were, as a whole, different to one other (Fig. S4). Analysis of the predicted
333 secondary structures of RNA I and RNA II highlighted similar sequence domains (stems and loops)
334 between pST1030-3 and NTP16; no conserved stems or loops were detected between pST1030-2A
335 and ColE1 or NTP16. The -35 and -10 sequences of RNAI and RNAII of pST1030-1A, pST1030-3
336 and ColE1 were conserved; the promoter sequence of NTP16 for RNAII was different. The
337 incompatibility determinants of ColE1-like plasmids are specific regions of RNA I/RNAII as
338 demonstrated by point mutations generated in the region of RNA I/ RNA II overlap or by the
339 different RNAI sequences that allowed ColE1 to coexist with RSF1030 a plasmid closely related to
340 NTP16 (Cannon and Strike, 1992; Tomizawa and Itoh, 1981). The presence of pST1030-2A and
341 pST1030-3 in the *Salmonella* strain ST1030 could then be explained by the different RNA I
342 sequences of these plasmids.

343 Searching for pST1030-2A sequence as query only produced a single record (plasmid
344 pSUH-5, Acc. N° CP041342) with a query cover of 100% (nucleotide identity \geq 95%). pSUH-5
345 was detected in *E. coli* isolated from human blood in Sweden in 2008. We also performed a search
346 using the *parA* sequence with a query cover of 100%. Apart from pSUH-5 where the nucleotide
347 identity for *parA* was 99,6%, results showed only nine records (Acc. N° CP043517; KU302809;

348 CP041060; CP036334; CP033951; CP035127; CP036324; CP023572; CP027113) with nucleotide
349 identity for *parA* ranging from 85,8 to 94,1 %. Records were from plasmids isolated from either *E.*
350 *coli*, *Klebsiella pneumoniae* or *Enterobacter* spp. All plasmids contained *oriV*-ColE1-like
351 sequences; the plasmids isolated from *Enterobacter* spp (Acc. N° CP043517; KU302809;
352 CP041060; CP023572; CP027113) also shared a partial nucleotide identity (from 88 to 94%) with
353 the ColE1 *oriT*. The pST1030-3 sequence was found to be nearly identical (99% identity, $\geq 99\%$
354 query cover) to six plasmids detected in *S. enterica* subsp. *enterica* (Acc. N° CP039594; CP033225;
355 MG948564; CP025235; CP025274; CP037878). The *Salmonella* strains were isolated between
356 2005 and 2013 from different sources and countries (Table S4).

357

358 3.4 Conjugation and transformation results

359 Results of conjugation experiments and PCR detection revealed the transfer of three distinct
360 resistance patterns (Table 1): i) CmSmSuTp (RU3) was transferred (pST1030-1A) with a mean
361 frequency of 3.1×10^{-3} transconjugants per donor (TC/D); ii) CmSmSuTcTp (RU3-RU2) was
362 transferred (plasmid pST1030-1B) with a mean frequency of 4.4×10^{-8} TC/D; iii)
363 ApCmSmSuTcTp (RU3-RU2-RU1) was transferred (plasmid pST1030-1C) with a mean frequency
364 of 6.6×10^{-9} TC/D. The transconjugant strains BA2A, BA2B and BA2C carrying the plasmids
365 pST1030-1A, pST1030-1B and pST1030-1C, respectively, were used as donors in conjugation
366 experiments with *E. coli* DH5 α Rf used as the recipient strain. pST1030-1B and pST1030-1C were
367 transferred with a mean frequency similar to that established for pST1030-1A (Table 1).

368

Table 1. Horizontal gene transfer

Strain	Resistance(s) ^a	Resistance genes	Genome localisation	Transconjugant/ Transformant strain (plasmid)	Resistance genes transferred by conjugation	Frequency of conjugation (SD) ^e	Resistance genes transferred by transformation
ST1030	ApCmSmSuTcTp	<i>dfrA12-aadA2-cmlA1-aadA1-sul3</i> <i>bla</i> _{TEM} - <i>strAB-sul2</i> ; <i>tetR(B)-tetA(B)</i>	pST1030-1A ^b Chromosome	BA2A (pST1030-1A)	<i>dfrA12-aadA2-cmlA1-aadA1-sul3</i>	3.1 (±2.7) x 10 ⁻³	
				BA2B (pST1030-1B ^b)	<i>dfrA12-aadA2-cmlA1-aadA1-sul3</i> ; <i>tetR(B)-tetA(B)</i>	4.4 (±4.6) x 10 ⁻⁸	
				BA2C (pST1030-1C ^b)	<i>dfrA12-aadA2-cmlA1-aadA1-sul3</i> ; <i>bla</i> _{TEM} - <i>strAB-sul2</i> ; <i>tetR(B)-tetA(B)</i>	6.6 (±1.3) x 10 ⁻⁸	
				BA2D (pST1030-2B ^c)			<i>dfrA12-aadA2-cmlA1-aadA1-sul3</i>
BA2A	CmSmSuTp	<i>dfrA12-aadA2-cmlA1-aadA1-sul3</i>	pST1030-1A	BA2E (pST1030-1A)	<i>dfrA12-aadA2-cmlA1-aadA1-sul3</i>	1.3 (±0.2) x 10 ⁻²	
BA2B	CmSmSuTcTp	<i>dfrA12-aadA2-cmlA1-aadA1-sul3</i> ; <i>tetR(B)-tetA(B)</i>	pST1030-1B	BA2F (pST1030-1B)	<i>dfrA12-aadA2-cmlA1-aadA1-sul3</i> ; <i>tetR(B)-tetA(B)</i>	4.0 (±0.7) x 10 ⁻²	
BA2C	ApCmSmSuTcTp	<i>dfrA12-aadA2-cmlA1-aadA1-sul3</i> ; <i>bla</i> _{TEM} - <i>strAB-sul2</i> ; <i>tetR(B)-tetA(B)</i>	pST1030-1C	BA2G (pST1030-1C)	<i>dfrA12-aadA2-cmlA1-aadA1-sul3</i> ; <i>bla</i> _{TEM} - <i>strAB-sul2</i> ; <i>tetR(B)-tetA(B)</i>	2.2 (±1.0) x 10 ⁻²	
BA2H	ApCmSmSuTp	<i>bla</i> _{TEM} - <i>strAB-sul2</i> ; <i>dfrA12-aadA2-cmlA1-aadA1-sul3</i>	pST1007-1D ^d pST1030-2B	BA2I (pST1007-1D)	<i>bla</i> _{TEM} - <i>strAB-sul2</i>	4.0 (±2.1) x 10 ⁻²	
				BA2L (pST1007-1D) (pST1030-2B)	<i>bla</i> _{TEM} - <i>strAB-sul2</i> <i>dfrA12-aadA2-cmlA1-aadA1-sul3</i>	2.0 (±1.3) x 10 ⁻³	
BA2D	CmSmSuTp	<i>dfrA12-aadA2-cmlA1-aadA1-sul3</i>	pST1030-2B	none	none	none	

371

372 ^a Ampicillin (Ap); Chloramphenicol (Cm); Streptomycin (Sm); Sulfamethoxazole (Su); Tetracycline (Tc); Trimethoprim (Tp)

373 ^b II plasmid

374 ^c ColE1-like plasmid

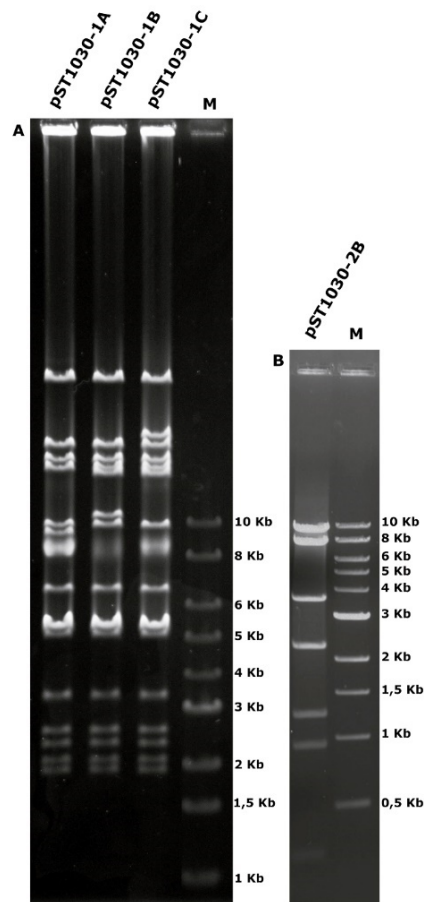
375 ^d FII plasmid

376 ^e Values represent the mean frequency (SD stands for Standard Deviation)

377 It was also proved possible to acquire the resistance pattern RU3 via transfor
378 BA2D). However, in this case the resistance markers were localised in the ColE1-lil
379 pST1030-2B.

380 Plasmid DNA (pST1030-1A, pST1030-1B and pST1030-1C) was extracted a
381 described and analysis of their restriction fragments revealed the presence of both a
382 and additional fragments for pST1030-1B and pST1030-1C (Fig. 4A, Table S3). Ov
383 highlighted pST1030-1A as the main conjugative plasmid harboured by ST1030; wh
384 1B and pST1030-1C were plasmids derived from pST1030-1A through acquisition o
385 RU2-RU1, respectively. By contrast, restriction patterns generated for pST1030-2B
386 different size and number to those of pST1030-1A (Fig. 4B, Table S3). The genetic
387 pST1030-1B and pST1030-1C were deduced by comparing their *ClaI*, *HindIII* and
388 with those of pST1030-1A and by specific PCRs (Fig. S1 and Table S2).

389



390

391
392 **Fig.4** Plasmid restriction patterns.
393 Plasmid names are reported above each line M: Quick Load 1 kb DNA Ladder (New England
394 Biolabs). **A)** *Clal* patterns. **B)** *EcoRI* pattern.
395

396 Mobilisation of pST1030-2B was assessed through conjugation experiments. pST1030-2B
397 was initially transferred into BA1D, a CSH26-Nal strain harbouring a conjugative FII plasmid
398 (pST1007-1D) that encodes resistance to ApSmSu. The strains BA2G (harbouring both pST1007-
399 1D and pST1030-2B) and BA2D (harbouring only pST1030-2B) were then used as donors in
400 conjugation experiments with DH5 α Rf. pST1030-2B was transferred only from matings with
401 BA2G (mean frequency of 2.0×10^{-3} TC/D) (Table 1).

402 We also investigated the co-transferring of pST1030-2A and/or pST1030-3 with pST1030-
403 1A. One hundred colonies selected on agar plates supplemented with both nalidixic acid and
404 trimethoprim, and from the maximal dilutions where transconjugants could be identified, were
405 analysed to detect the presence of pST1030-2A and/or pST1030-3. The presence of pST1030-2A
406 and pST1030-3 was established by enzyme restriction of the plasmid content from each analysed
407 transconjugant and by PCR detection with specific primers targeting pST1030-2A or pST1030-3
408 (Table S2). pST1030-2A was co-transferred in 92% of transconjugants; pST1030-2A and pST1030-
409 3 were both co-transferred in 56% of transconjugants; in 8% of transconjugants pST1030-1A was
410 found to be singularly transferred. pST1030-3 was never found co-transferred alone.

411 The average generation-time, estimated at 21 min for the transconjugant BA2A (harbouring
412 only pST1030-1A), BA2M (harbouring the additional pST1030-2A) and BA2N (harbouring both
413 pST1030-2A and pST1030-3) (Table S5) led us to deduce that the presence of ColE1-like plasmids
414 in transconjugants harbouring pST1030-1A seems not to affect their fitness cost.

415

416 **4. Discussions**

417 *S. Typhimurium* is one of the most commonly isolated serovars from humans, retail meats of
418 diverse origins and the environment. It has arguably the broadest host and pathogenicity range of all

419 serovars of *S. enterica* subsp. *enterica* (Paul et al., 2016). Its broad host-range spectrum exposes this
420 serovar to a wide potential inflow and outflow of horizontally transmitted genetic elements such as
421 plasmids. These last elements, as well as IS and Tn, are reported to play a key role in the spreading
422 of ARGs and in the insurgence of MDR strains; the latter is now acknowledged as one of the
423 emerging and most feared public health threats on a worldwide scale (Tanwar et al., 2014). In
424 addition to conjugative plasmids, HGT of ARGs can also be mediated by non-conjugative
425 mobilisable plasmids. The contribution of these plasmids is a matter of growing interest and
426 research studies (Oliva et al., 2017; Ramsay and Firth, 2017; Rozwandowicz et al., 2018; Suhartono
427 et al., 2018).

428 ST1030 is an MDR STMV strain that contains: i) two chromosomal RUs conferring
429 resistance to ApSmSu (RU1) and Tc (RU2); ii) one conjugative I1 plasmid (pST1030-1A)
430 harbouring a Tn21-derived element that confers resistance to CmSmSuTp (RU3); iii) two ColE1-
431 like plasmids of which one mobilisable (pST1030-2A) and one identified as orphan *mob*-associated
432 *oriT* (pST1030-3). This study has further highlighted the role played by IS26 elements in the spread
433 of ARGs. In ST1030, they mediated gene shuffling that generated a pool of conjugative I1 plasmids
434 harbouring diverse sets of ARGs: *dfrA12-aadA2-cmlA1-aadA1-sul3* (pST1030-1A), *dfrA12-aadA2-*
435 *cmlA1-aadA1-sul3-tetR(B)-tetA(B)* (pST1030-1B) and *dfrA12-aadA2-cmlA1-aadA1-sul3- tetR(B)-*
436 *tetA(B) bla_{TEM-1}-sul2-strAB* (pST1030-1C). Transconjugants exhibiting resistance RU3-RU1 were
437 not detected. It is possible that the absence of their detection might be due to a low frequency of
438 formation of the cointegrate RU3-RU1. Moreover, the IS26-mediated gene shuffling also generated
439 diverse Tn21-derived elements that might further spread the harboured ARGs within other bacterial
440 genomes by intracellular translocation. pST1030-1A also shares an identical fragment C with a
441 Tn21-derived element inserted into the same nucleotide position of *ydfA* with pST1007-1A (a
442 mosaic FII conjugative plasmid isolated from the *S. Typhimurium* strain ST1007 collected in
443 Apulia during the same, 2006-2008, three-year period) and, with the presence of a conserved
444 (TSD), this suggests a possible recent insertion of this element. The fragment C can only be

445 detected, *in silico*, in I1 plasmids and we previously hypothesised that its presence in pST1007-1A
446 reflected acquisition from I1 plasmids (Oliva et al., 2018). This hypothesis is further supported by
447 the present study. A comparative analysis of the RUs between ST1030 and ST1007 showed the
448 presence of two mismatches in RU1 (of which one determined the replacement of the glutamic acid
449 at position 212 of StrA of ST1007 by an aspartic acid in ST1030); in RU2 the Δ IS10-left sequence
450 of ST1030 (250bp) was shorter than that in ST007 (340bp) and also the RU2 of ST1030 lacked the
451 sequence spanning from *merR* to the *AtniA* of the Tn21-derived element; the RU3 of both were
452 identical.

453 The mobilisable pST1030-2A ColE1-like plasmid was efficiently co-transferred (92% of the
454 analysed transconjugants) by pST1030-1A. The transfer efficiency of pST1030-2A mediated by
455 pST1030-1A was higher than that reported for some ColE1-like plasmids such as NTP1 and NTP16
456 (frequency from 50 to 60%) co-transferred by R64 (Lambert et al., 1987), or by other plasmids
457 harbouring *oriT*-like sequences of the co-resident conjugative plasmids (e.g pBuzz was co-
458 transferred with an efficiency of 70% by the co-resident Inc B/O p838B-R plasmid) (Moran and
459 Hall, 2019). pST1030-2A was also the target of an intracellular translocation of the Tn21-derived
460 element. This generated the pST1030-2B plasmid encoding for multidrug resistance. The Tn21-
461 derived element became inserted into *mbeC* and a potential new promoter between the Tn21-IR_{mer}
462 and the TSD was formed. This might allow transcription of Δ *mbeC* whose translated product
463 (Δ MbeC) would retain the C-terminal function required to bind the N-terminal region of MbeA
464 relaxase. However, Δ MbeC would not retain the N-terminal function possibly necessary to bind an
465 *oriT* sequence next to the *nic* site. The horizontal transfer of pST1030-2B by the conjugative FII
466 plasmid pST1007-1D raises open questions as to the possible role played by either the absence of
467 MbeC or the presence of a Δ MbeC in the mobilisation of pST1030-2B. Moreover, pST1030-2A
468 carries *parA* whose encoded protein is ascribable to “orphan ParAs” that are not associated with the
469 usual partner ParB (Lutkenhaus, 2012). Actually, in addition to the three types of classical plasmid
470 segregation systems there are data emerging that support the presence of other, as yet unknown,

471 mechanisms that can ensure plasmid partitioning in each daughter cell during division (Guynet and
472 de la Cruz, 2011). Whether the presence of *parA* in pST1030-2A is somehow related to a new
473 segregation system remains to be explored.

474 The other identified ColE1-like plasmid (pST1030-3) was an orphan *mob*-associated *oriT*
475 element. It lacked *mob* genes but harboured sequences of which one was nearly identical to ColE1
476 and pST1030-2A *oriT* and one similar to pST1030-1A and R64 *oriT*. pST1030-3 was co-transferred
477 with pST1030-1A and pST1030-2A in 56% of transconjugants harbouring these plasmids. In
478 addition to mobilisable plasmids, those lacking Mob relaxase (conventionally described as non-
479 mobilisable) may be mobilised *in trans* by conjugative elements if carrying a mimic of the
480 conjugative element's *oriT* sequence (Ramsay and Firth, 2017). *oriT* mimicry plasmids have
481 recently been described in *Staphylococcus* (Ramsay et al., 2016), *E. coli* (Moran and Hall, 2019),
482 *Acinetobacter baumannii* (Blackwell and Hall, 2019) and *Citrobacter freundii* (Barry et al., 2019).
483 Some *oriT* mimicry plasmids may also carry relaxosome accessory factors as reported for pCERC7
484 (a plasmid isolated in *E. coli*) that can be mobilised by R64 (Moran and Hall, 2017). Other non-
485 mobilisable plasmids are defined as orphan *mob*-associated *oriT* (Ramsay and Firth, 2017).
486 Mobilisation of these plasmids requires both a conjugative element and a *mob*-gene-carrying
487 element. pST1030-3 is undoubtedly an orphan *mob*-associated *oriT* plasmid and, to the best of our
488 knowledge, this is the first report (at least in *Salmonella*) of a natural isolate harbouring a three-
489 element mobilisation system in the same cell. pST1030-3 also carries a Type III restriction
490 modification (R-M) system. Type III R-M systems are present in a large number of sequenced
491 bacterial genomes (Rao et al., 2014). The widespread nature of these systems indicates their
492 importance, despite many aspects of their biological function remaining to be established. Whether
493 the presence of a Type III R-M system in pST1030-3 confers a mutual benefit for both plasmid and
494 host or merely a plasmid benefit remains to be explored.

495 In most STMV strains isolated worldwide from humans, animals, foods and environmental
496 sources an IS26 copy was detected next to *iroB* (Boland et al., 2018). This suggested a possible

497 common ancestor for the globally observed STMV identified in recent years. It has thus been
498 proposed that insertion and recombination of IS26 elements has probably been the driving force
499 behind the genetic variability of the STMV population (Boland et al., 2018). However, in ST1030
500 the IS26 element next to *iroB* is interrupted by an *IS1* element. *IS1*-mediated intramolecular
501 rearrangements have been documented (Turlan and Chandler, 1995) and the ST1030 chromosome
502 harbours five *IS1* elements of which one has a perfect TSD, indicating the presence of a recent *IS1*
503 integration. We cannot exclude the possibility that an *IS1*-mediated deletion between the *IS1*
504 present in the Tn21-derived element and an *IS1* copy inserted into the IS26, originally next to *iroB*,
505 triggered the loss of the chromosomal region from 3' STM2759 to *fljA-fljB-hin*.

506 The present study, in our view, reinforces the role played by different genetic elements in
507 the spread of ARGs. It also supplies new data on features harboured by non-conjugative plasmids
508 that increasingly emerge as a dynamic and complex group of the fascinating world of plasmids.

509

510 **Acknowledgements**

511 Very many thanks to thank Karen Laxton for writing assistance. Special thanks are also due
512 to Dr. Francesca Fanelli (ISPA-CNR) and Dr. Cosma Liuzzi for preparing libraries and sequencing.

513

514 **References**

- 515 Antunes, P., et al., 2007. Dissemination of sul3-containing elements linked to class 1 integrons with
516 an unusual 3' conserved sequence region among Salmonella isolates. Antimicrob Agents
517 Chemother. 51, 1545-8.
- 518 Bankevich, A., et al., 2012. SPAdes: a new genome assembly algorithm and its applications to
519 single-cell sequencing. J Comput Biol. 19, 455-77.
- 520 Barry, K. E., et al., 2019. Don't overlook the little guy: An evaluation of the frequency of small
521 plasmids co-conjugating with larger carbapenemase gene containing plasmids. Plasmid. 103,
522 1-8.

523 Blackwell, G. A., Hall, R. M., 2019. Mobilisation of a small *Acinetobacter* plasmid carrying an oriT
524 transfer origin by conjugative RepAci6 plasmids. *Plasmid*. 103, 36-44.

525 Boland, C., et al., 2018. A liquid bead array for the identification and characterization of fljB-
526 positive and fljB-negative monophasic variants of *Salmonella* Typhimurium. *Food*
527 *microbiology*. 71, 17-24.

528 Brantl, S., 2014. Plasmid Replication Control by Antisense RNAs. *Microbiol Spectr*. 2, PLAS-
529 0001-2013.

530 Brouwer, M. S., et al., 2015. IncI shufflons: Assembly issues in the next-generation sequencing era.
531 *Plasmid*. 80, 111-7.

532 Cain, A. K., Hall, R. M., 2012. Evolution of a multiple antibiotic resistance region in IncHI1
533 plasmids: reshaping resistance regions in situ. *The Journal of antimicrobial chemotherapy*.
534 67, 2848-53.

535 Camarda, A., et al., 2013. Resistance genes, phage types and pulsed field gel electrophoresis
536 pulsotypes in *Salmonella enterica* strains from laying hen farms in southern Italy.
537 *International journal of environmental research and public health*. 10, 3347-62.

538 Cambray, G., et al., 2010. Integrons. *Annu Rev Genet*. 44, 141-66.

539 Camps, M., 2010. Modulation of ColE1-like plasmid replication for recombinant gene expression.
540 *Recent Pat DNA Gene Seq*. 4, 58-73.

541 Cannon, P. M., Strike, P., 1992. Complete nucleotide sequence and gene organization of plasmid
542 NTP16. *Plasmid*. 27, 220-30.

543 Carattoli, A., et al., 2005. Identification of plasmids by PCR-based replicon typing. *Journal of*
544 *microbiological methods*. 63, 219-28.

545 Chan, P. T., et al., 1985. Nucleotide sequence and gene organization of ColE1 DNA. *The Journal of*
546 *biological chemistry*. 260, 8925-35.

547 Curiao, T., et al., 2011. Association of composite IS26-sul3 elements with highly transmissible
548 IncI1 plasmids in extended-spectrum-beta-lactamase-producing *Escherichia coli* clones from
549 humans. *Antimicrobial Agents and Chemotherapy*. 55, 2451-7.

550 De Vito, D., et al., 2015. Diffusion and persistence of multidrug resistant *Salmonella* Typhimurium
551 strains phage type DT120 in southern Italy. *Biomed Res Int*. 2015, 265042.

552 Domingues, S., et al., 2015. Global dissemination patterns of common gene cassette arrays in class
553 1 integrons. *Microbiology*. 161, 1313-37.

554 Echeita, M. A., et al., 2001. Atypical, fljB-negative *Salmonella enterica* subsp. *enterica* strain of
555 serovar 4,5,12:i:- appears to be a monophasic variant of serovar Typhimurium. *Journal of*
556 *clinical microbiology*. 39, 2981-3.

557 Foster, T. J., et al., 1981. Genetic organization of transposon Tn10. *Cell*. 23, 201-13.

558 Furuya, N., Komano, T., 1997. Mutational analysis of the R64 oriT region: requirement for precise
559 location of the NikA-binding sequence. *J Bacteriol*. 179, 7291-7.

560 Gruber, A. R., et al., 2008. The Vienna RNA websuite. *Nucleic acids research*. 36, W70-4.

561 Guynet, C., de la Cruz, F., 2011. Plasmid segregation without partition. *Mobile genetic elements*. 1,
562 236-241.

563 Hall, R. M., Collis, C. M., 1995. Mobile gene cassettes and integrons: capture and spread of genes
564 by site-specific recombination. *Molecular microbiology*. 15, 593-600.

565 Harmer, C. J., Hall, R. M., 2015. IS26-Mediated Precise Excision of the IS26-aphA1a
566 Translocatable Unit. *MBio*. 6, e01866-15.

567 Harmer, C. J., Hall, R. M., 2016. IS26-Mediated Formation of Transposons Carrying Antibiotic
568 Resistance Genes. *mSphere*. 1.

569 Harmer, C. J., Hall, R. M., 2017. Targeted conservative formation of cointegrates between two
570 DNA molecules containing IS26 occurs via strand exchange at either IS end. *Molecular*
571 *microbiology*. 106, 409-418.

572 Harmer, C. J., et al., 2014. Movement of IS26-associated antibiotic resistance genes occurs via a
573 translocatable unit that includes a single IS26 and preferentially inserts adjacent to another
574 IS26. *MBio.* 5, e01801-14.

575 He, S., et al., 2015. Insertion Sequence IS26 Reorganizes Plasmids in Clinically Isolated Multidrug-
576 Resistant Bacteria by Replicative Transposition. *MBio.* 6.

577 Klucar, L., et al., 2010. phiSITE: database of gene regulation in bacteriophages. *Nucleic acids*
578 *research.* 38, D366-70.

579 Lambert, C. M., et al., 1987. Conjugal mobility of the multicopy plasmids NTP1 and NTP16.
580 *Plasmid.* 18, 99-110.

581 Leipe, D. D., et al., 2002. Classification and evolution of P-loop GTPases and related ATPases.
582 *Journal of molecular biology.* 317, 41-72.

583 Liebert, C. A., et al., 1999. Transposon Tn21, flagship of the floating genome. *Microbiology and*
584 *molecular biology reviews : MMBR.* 63, 507-22.

585 Lorenz, R., et al., 2011. ViennaRNA Package 2.0. *Algorithms Mol Biol.* 6, 26.

586 Lutkenhaus, J., 2012. The ParA/MinD family puts things in their place. *Trends in microbiology.* 20,
587 411-8.

588 Lutkenhaus, J., Sundaramoorthy, M., 2003. MinD and role of the deviant Walker A motif,
589 dimerization and membrane binding in oscillation. *Molecular microbiology.* 48, 295-303.

590 Madeira, F., et al., 2019. The EMBL-EBI search and sequence analysis tools APIs in 2019. *Nucleic*
591 *acids research.* 47, W636-W641.

592 Marchler-Bauer, A., et al., 2017. CDD/SPARCLE: functional classification of proteins via
593 subfamily domain architectures. *Nucleic acids research.* 45, D200-D203.

594 Miriagou, V., et al., 2006. Antimicrobial resistance islands: resistance gene clusters in *Salmonella*
595 chromosome and plasmids. *Microbes and infection / Institut Pasteur.* 8, 1923-30.

596 Mollet, B., et al., 1985. Gene organization and target specificity of the prokaryotic mobile genetic
597 element IS26. *Molecular & general genetics : MGG.* 201, 198-203.

598 Moran, R. A., Hall, R. M., 2017. Analysis of pCERC7, a small antibiotic resistance plasmid from a
599 commensal ST131 *Escherichia coli*, defines a diverse group of plasmids that include various
600 segments adjacent to a multimer resolution site and encode the same NikA relaxase
601 accessory protein enabling mobilisation. *Plasmid*. 89, 42-48.

602 Moran, R. A., Hall, R. M., 2018. Evolution of Regions Containing Antibiotic Resistance Genes in
603 FII-2-FIB-1 ColV-Colla Virulence Plasmids. *Microbial drug resistance*. 24, 411-421.

604 Moran, R. A., Hall, R. M., 2019. pBuzz: A cryptic rolling-circle plasmid from a commensal
605 *Escherichia coli* has two inversely oriented oriTs and is mobilised by a B/O plasmid.
606 *Plasmid*. 101, 10-19.

607 Moran, R. A., et al., 2016. pCERC3 from a commensal ST95 *Escherichia coli*: A ColV virulence-
608 multiresistance plasmid carrying a sul3-associated class 1 integron. *Plasmid*. 84-85, 11-9.

609 Murray, M. G., Thompson, W. F., 1980. Rapid isolation of high molecular weight plant DNA.
610 *Nucleic acids research*. 8, 4321-5.

611 Oliva, M., et al., 2018. IS26 mediated antimicrobial resistance gene shuffling from the chromosome
612 to a mosaic conjugative FII plasmid. *Plasmid*. 100, 22-30.

613 Oliva, M., et al., 2017. A novel group of IncQ1 plasmids conferring multidrug resistance. *Plasmid*.
614 89, 22-26.

615 Partridge, S. R., et al., 2018. Mobile Genetic Elements Associated with Antimicrobial Resistance.
616 *Clin Microbiol Rev*. 31.

617 Partridge, S. R., et al., 2009. Gene cassettes and cassette arrays in mobile resistance integrons.
618 *FEMS microbiology reviews*. 33, 757-84.

619 Paul, S., et al., 2016. Corrected Genome Annotations Reveal Gene Loss and Antibiotic Resistance
620 as Drivers in the Fitness Evolution of *Salmonella enterica* Serovar Typhimurium. *J*
621 *Bacteriol*. 198, 3152-3161.

622 Ramsay, J. P., Firth, N., 2017. Diverse mobilization strategies facilitate transfer of non-conjugative
623 mobile genetic elements. *Current opinion in microbiology*. 38, 1-9.

624 Ramsay, J. P., et al., 2016. An updated view of plasmid conjugation and mobilization in
625 *Staphylococcus*. *Mobile genetic elements*. 6, e1208317.

626 Rao, D. N., et al., 2014. Type III restriction-modification enzymes: a historical perspective. *Nucleic*
627 *acids research*. 42, 45-55.

628 Reid, C. J., et al., 2015. Tn6026 and Tn6029 are found in complex resistance regions mobilised by
629 diverse plasmids and chromosomal islands in multiple antibiotic resistant
630 *Enterobacteriaceae*. *Plasmid*. 80, 127-37.

631 Roberts, R. J., et al., 2015. REBASE--a database for DNA restriction and modification: enzymes,
632 genes and genomes. *Nucleic acids research*. 43, D298-9.

633 Rozwandowicz, M., et al., 2018. Plasmids carrying antimicrobial resistance genes in
634 *Enterobacteriaceae*. *The Journal of antimicrobial chemotherapy*.

635 Sampei, G., et al., 2010. Complete genome sequence of the incompatibility group I1 plasmid R64.
636 *Plasmid*. 64, 92-103.

637 Seemann, T., 2014. Prokka: rapid prokaryotic genome annotation. *Bioinformatics*. 30, 2068-9.

638 Shimada, T., et al., 2014. The whole set of constitutive promoters recognized by RNA polymerase
639 RpoD holoenzyme of *Escherichia coli*. *PloS one*. 9, e90447.

640 Smillie, C., et al., 2010. Mobility of plasmids. *Microbiology and molecular biology reviews* :
641 *MMBR*. 74, 434-52.

642 Stokes, H. W., Gillings, M. R., 2011. Gene flow, mobile genetic elements and the recruitment of
643 antibiotic resistance genes into Gram-negative pathogens. *FEMS microbiology reviews*. 35,
644 790-819.

645 Suhartono, S., et al., 2018. Transmissible Plasmids and Integrons Shift *Escherichia coli* Population
646 Toward Larger Multiple Drug Resistance Numbers. *Microbial drug resistance*. 24, 244-252.

647 Tanwar, J., et al., 2014. Multidrug resistance: an emerging crisis. *Interdiscip Perspect Infect Dis*.
648 2014, 541340.

649 Tomizawa, J., Itoh, T., 1981. Plasmid ColE1 incompatibility determined by interaction of RNA I
650 with primer transcript. Proceedings of the National Academy of Sciences of the United
651 States of America. 78, 6096-100.

652 Turlan, C., Chandler, M., 1995. IS1-mediated intramolecular rearrangements: formation of excised
653 transposon circles and replicative deletions. The EMBO journal. 14, 5410-21.

654 Varsaki, A., et al., 2012. Interaction between relaxase MbeA and accessory protein MbeC of the
655 conjugally mobilizable plasmid ColE1. FEBS Lett. 586, 675-9.

656 Varsaki, A., et al., 2009. Analysis of ColE1 MbeC unveils an extended ribbon-helix-helix family of
657 nicking accessory proteins. J Bacteriol. 191, 1446-55.

658 Zheng, W., et al., 2020. Clinical class 1 integron-integrase gene - A promising indicator to monitor
659 the abundance and elimination of antibiotic resistance genes in an urban wastewater
660 treatment plant. Environment international. 135, 105372.